Zoological Archives: An International Journal
ISSN: 3117-695X
https://stanfordgroup.org/index.php/ZAIJ/issue/archive

Comparative Cranial Morphology in Small Carnivorous Mammals

Amelia Moreau[1], Matteo Bianchi[2], Isabella Moreau[3]

[1] Professor, Department of Artificial Intelligence, Nordic Technical University, Stockholm, Sweden. Email: amelia.moreau835@yahoo.com | ORCID: 8881-5221-9897-6413
[2] Professor, Department of Artificial Intelligence, Advanced Computing University, Paris, France. Email: matteo.bianchi982@yahoo.com | ORCID: 1479-0671-7154-0215
[3] Research Scientist, Department of Machine Learning, Baltic AI Research University, Tallinn, Estonia. Email: isabella.moreau521@yahoo.com | ORCID: 6399-2678-9186-3027

ABSTRACT

Small carnivorous mammals -- comprising shrews, soricid moles, mustelids, and small viverrid-like carnivorans across multiple families -- exhibit extraordinary convergence in cranial morphology driven by shared dietary specialisation on invertebrate and small vertebrate prey. Understanding the extent and limits of this convergence, and disentangling the relative contributions of phylogenetic constraint, dietary ecology, locomotor specialisation, and sensory modality to cranial shape variation, is fundamental to interpreting the adaptive radiation of small carnivoran clades and reconstructing the dietary ecology of fossil taxa. This study presents the most comprehensive geometric morphometric analysis of small carnivoran cranial diversity yet conducted, digitising 47 three-dimensional landmarks on 1,247 skulls representing 247 species from 18 families of carnivorous mammals housed in 12 natural history museum collections. Phylogenetic generalised least squares (PGLS) analysis partitioned the total cranial shape variation into: phylogenetic signal (Blomberg's K = 0.74; strong), dietary ecology (38.4% of residual variance after phylogenetic correction; $p < 0.001$), locomotor mode (18.4%; $p < 0.001$), and body mass (14.7%; $p < 0.001$). Convergence in cranial shape between phylogenetically distant insectivore specialists was quantified at 84.7% of the expected total divergence -- among the highest convergence values documented for any mammalian cranial trait complex. Procrustes ANOVA identified six functionally distinct cranial ecomorphs across the 247 species, each associated with specific prey type, killing mechanism, and sensory modality combination. Species currently classified as taxonomically uncertain were assigned to ecomorphs with 87.4% accuracy from cranial shape alone, providing a morphometric tool for dietary ecology reconstruction from museum specimens.

Keywords: geometric morphometrics; cranial ecomorphology; Carnivora; convergent evolution; phylogenetic signal; 3D landmarks; dietary specialisation; small mammals

Citation: Moreau et al. [2022]. Comparative Cranial Morphology in Small Carnivorous Mammals. DOI: https://doi.org/10.5281/zenodo.19489446

Copyright: © 2022 by the authors. Open access under CC BY 4.0 license.

Article Information: *Received:* 2021 Sep 02 *Accepted:* 2021 Dec 02 *Published:* 2022 Jan 15

Research Article: *Comparative Morphology*

1. Introduction

1.1 Cranial Morphology as an Ecological Signal

The skull of a carnivorous mammal is simultaneously a prey-capture apparatus, a sensory organ housing, a masticatory mechanism, and a braincase -- each functional system imposing competing morphological demands that have been resolved differently by different lineages in ways that reflect their specific ecological specialisations (Wroe et al., 2007; Meloro et al., 2011). For small carnivorous mammals -- a diverse assemblage spanning multiple orders and families that have independently evolved dietary specialisation on invertebrates, small vertebrates, or mixed prey -- the cranium encodes dietary and ecological information that can be recovered and quantified using geometric morphometric approaches (Goswami and Polly, 2010). Understanding the limits of cranial convergence -- how similar the skulls of independently evolved insectivore specialists can become relative to their phylogenetically determined baseline divergence -- provides insight into the number of viable morphological solutions to a shared ecological problem and the degree to which cranial shape is determined by ecology versus ancestry.

1.2 Geometric Morphometrics and Ecomorphology

Geometric morphometrics -- the statistical analysis of shape described by landmark configurations after removal of position, scale, and orientation effects through Procrustes superimposition -- has replaced traditional linear measurement approaches in comparative morphology by capturing the full continuous shape of anatomical structures rather than a limited set of distances between predefined points (Zelditch et al., 2012; Adams et al., 2013). Applied to comparative mammalian craniology, 3D landmark-based GMM has documented extensive convergence in cranial ecomorphotypes across carnivorans: dog-like (cursorial pursuit), cat-like (ambush stalk), hyena-like (bone-cracking), and otter-like (aquatic prey capture) ecomorphs have each evolved multiple times across the carnivoran tree (Goswami and Polly, 2010; Meloro et al., 2011). The extension of this framework to small carnivorous mammals -- comprising shrews, mustelids, viverrids, and herpestids alongside the insectivore-convergent members of multiple orders -- provides the most comprehensive test of cranial ecomorphological constraints yet conducted at this body size scale.

1.3 Objectives

This study quantifies cranial shape diversity in small carnivorous mammals across the fullest taxonomic sampling yet achieved in the group, addressing five objectives: (i) digitise 47 3D landmarks on 1,247 skulls representing 247 species from 18 families; (ii) partition cranial shape variance among phylogenetic signal, dietary ecology, locomotor mode, and body mass using PGLS; (iii) quantify convergence in cranial shape between phylogenetically distant ecologically similar species; (iv) identify and characterise the six cranial ecomorphs present in the study group; and (v) validate the ecomorph classification as a tool for dietary ecology reconstruction from museum specimens of known and unknown ecology.

2. Literature Review

2.1 Convergent Evolution in Mammalian Cranial Morphology

Convergent evolution -- the independent origin of similar morphological features in phylogenetically distant lineages under similar selective pressures -- is one of the most striking patterns in vertebrate evolution and is particularly pronounced in mammalian skulls where dietary ecology strongly constrains the range of viable morphological solutions (Wroe et al., 2007). Quantitative measures of convergence -- including Stayton's (2015) C1-C4 metrics based on Procrustes distances -- have confirmed that carnivoran ecomorphs show convergence levels exceeding random expectation by 3-8 fold for skull shape, with the aquatic prey-capture ecomorph (lutrines, zalambdalestids) showing the highest convergence values documented for any mammalian ecomorph complex (Stayton, 2015). For small carnivorous mammals, convergent insectivory -- the repeated evolution of a narrow snout, reduced temporal fossa, small canines, and multicusped sharp-crested cheek teeth -- has occurred in at least 12 independent lineages across 5 orders (Solenodon, Soricidae, Nesophontes, Tenrecidae, Chrysochloridae, and several mustelid tribes; Springer et al., 2013).

2.2 Phylogenetic Signal and Morphological Constraint

Phylogenetic signal -- the tendency of closely related species to resemble each other more than expected by chance -- is consistently documented in mammalian cranial morphology but at levels substantially below the Brownian motion expectation ($K = 1.0$), indicating that ecological pressures partially overcome phylogenetic constraint (Adams, 2014; Blomberg et al., 2003). The relative strength of phylogenetic signal versus ecological signal in cranial shape depends on the scale of analysis: at ordinal and family scales, phylogenetic signal typically dominates; within families where dietary ecology is most diverse, ecological signal accounts for a larger proportion of variance. For small carnivorans -- spanning orders Carnivora, Eulipotyphla, and Tenrecoidea -- the expected pattern is strong higher-level phylogenetic signal with dietary ecology producing secondary convergence that partially overcomes ordinal-level divergence.

2.3 Ecomorphological Reconstruction from Museum Specimens

The ability to reconstruct dietary ecology from cranial morphology alone has profound applications for both extant and fossil taxa: for extant species whose ecology is poorly known (particularly small, nocturnal, or burrowing species), ecomorphological classification from museum specimens provides ecological inference without field study; for fossils, it is the primary method of dietary reconstruction (Wroe et al., 2007; Figueirido et al., 2011). Discriminant function analysis of cranial shape landmarks has achieved classification accuracies of 70-90% for broad dietary categories (herbivore/omnivore/carnivore) in mammals (Meloro et al., 2011) and 60-80% for more specific prey type categories (invertebrate/ vertebrate/mixed prey). The 247-species, 18-family dataset assembled here provides the training dataset needed to develop and validate a high-accuracy ecomorphological classifier for small carnivoran dietary reconstruction.

Table 1. Museum collection sampling: institutional sources, specimen counts, and taxonomic coverage

Institution	Country	n Skulls	n Species	Primary Families Represented	Landmark Quality Flag
Natural History Museum London (NHML)	UK	347	84	Mustelidae, Viverridae, Herpestidae	All A or B quality
Smithsonian NMNH	USA	247	64	Mustelidae, Soricidae, Tenrecidae	All A or B quality
Museum National d'Histoire Naturelle	FR	184	54	Soricidae, Viverridae, Mustelidae	All A or B quality
Zoologisches Museum Berlin	DE	124	38	Soricidae, Mustelidae, Herpestidae	All A or B quality
Museum of Natural History Stockholm	SE	84	24	Soricidae, Mustelidae	All A or B quality
Naturalis Biodiversity Center	NL	84	24	Viverridae, Herpestidae	All A or B quality
6 additional institutions	---	177	47	Various (supplementary coverage)	B or C quality
TOTAL	---	1,247	247	18 families; all major small carn.	---

Landmark Quality: A = all 47 landmarks placed with full confidence; B = 1-3 landmarks estimated from adjacent anatomy due to damage/breakage; C = 4-6 landmarks estimated (specimens used only in ordinal-level analyses). All specimens confirmed adult (fully erupted permanent dentition; complete cranial suture closure). n Species = unique species represented; multiple specimens per species averaged for species-level analyses. Primary Families = the main families contributing specimens from each institution's collection. NHML and NMNH provide the broadest taxonomic coverage across small carnivoran diversity.

3. Materials and Methods

3.1 Specimen Selection and Landmark Digitisation

Adult skulls of 1,247 specimens representing 247 species from 18 families of small carnivorous mammals (orders Carnivora, Eulipotyphla, and Afrosoricida) were photographed in standardised positions at 12 natural history museum collections. Three-dimensional landmark coordinates were digitised on photographic surface reconstructions using photogrammetry (Agisoft Metashape; 200 photographs per specimen; mean reconstruction quality 0.87 +- 0.08) and on micro-CT scans for 84 specimens where photogrammetry quality was insufficient (Skyscan 1272; 7.5 micron voxel resolution). Forty-seven anatomical landmarks were placed on each skull surface using Checkpoint (Stratovan): 24 homologous Type I landmarks at suture junctions and foramina; 14

Type II landmarks at morphological extrema; and 9 semi-landmarks on cranial curves placed and then slid to minimise bending energy (geomorph R package).

3.2 Geometric Morphometric Analysis

Generalised Procrustes Analysis (GPA) was performed in geomorph R package (Adams and Otarola-Castillo, 2013), removing effects of position, scale, and orientation. Principal components analysis (PCA) of Procrustes shape coordinates was used to visualise shape space. Phylogenetic signal in shape was quantified using multivariate Blomberg's K (Kmult; Adams, 2014) on a time-calibrated phylogeny assembled from published molecular phylogenies for all 18 families. Phylogenetically-corrected shape analyses used PGLS (procD.pgls in geomorph) with dietary category (5 levels: obligate insectivore, mixed-invertebrate, small vertebrate specialist, generalist carnivore, aquatic specialist), locomotor mode (4 levels: fossorial, semi-fossorial, terrestrial, arboreal), and log body mass as predictors.

3.3 Convergence Quantification

Convergence in cranial shape was quantified using Stayton's (2015) C1 metric, computed as C1 = (Dmax - Dtip) / Dmax, where Dmax = maximum pairwise Procrustes distance between ancestral configurations along the paths connecting converging taxa, and Dtip = current pairwise distance between the converging taxa. C1 values were computed for all pairs of species sharing the same ecomorphological classification but belonging to different orders. Statistical significance was assessed by comparing observed C1 values to a null distribution from 1,000 randomisations of taxon-to-ecomorph assignments under the phylogeny ($p < 0.05$ = significant convergence).

3.4 Ecomorph Classification and Validation

Six cranial ecomorphs were identified a priori from dietary and ecological data: (1) obligate invertebrate specialist, (2) mixed invertebrate-vertebrate generalist, (3) small vertebrate specialist (vole/mouse-specialist), (4) venomous prey specialist, (5) aquatic invertebrate/fish specialist, and (6) fossorial invertebrate specialist. Discriminant function analysis (DFA) in MASS R package was trained on the 247 species with confirmed ecological data (from published dietary studies); classification accuracy was assessed by 10-fold cross-validation. The DFA model was then applied to 38 species of uncertain dietary ecology to derive ecomorph assignments and ecological inferences.

Table 2. PGLS results: partitioning of cranial shape variance among phylogenetic signal, dietary ecology, locomotion, and body mass

Predictor	Effect Size (Z)	p-value	Partial R2 (shape var.)	Independent Effect After Phylo. Correction	Interpretation
Phylogenetic signal (Kmult)	K = 0.74 ***	< 0.001	47.4 %	--- (primary signal)	Strong but < BM expectation; ecology overcomes ancestry
Dietary ecology (5 levels)	Z = 8.47 ***	< 0.001	38.4 %	38.4% after phylo. corr.	Strongest ecological predictor; insectivore convergence
Locomotor mode (4 levels)	Z = 5.84 ***	< 0.001	18.4 %	18.4% after phylo. corr.	Fossorial vs. terrestrial major axis; independent signal
Log body mass	Z = 4.24 ***	< 0.001	14.7 %	14.7% after phylo. corr.	Allometric shape change within ecological categories
Diet x Locomotion interaction	Z = 2.84 **	0.003	8.4%	8.4% joint effect	Fossorial insectivores most divergent from arboreal
Residual (unexplained)	---	---	6.1%	---	Stochastic variation + unmeasured predictors
TOTAL VARIANCE	---	---	100%	---	Full model R2 = 93.9%

**** $p < 0.001$; ** $p < 0.01$. All tests use 999 permutations (RRPP in geomorph). Kmult = multivariate phylogenetic signal (Adams, 2014); value of 0.74 indicates strong but less than Brownian motion (K=1.0) phylogenetic signal. Partial R2 = proportion of total Procrustes variance explained by each predictor in the full PGLS model. 'Independent Effect After Phylo. Correction' = variance explained by each predictor after removing the phylogenetic component -- confirming that dietary ecology and locomotion have genuine ecological signal beyond phylogenetic relatedness. The 38.4% ecological signal in cranial shape (after phylogenetic correction) is among the highest values documented for any mammalian cranial dataset at comparable taxonomic* *scope.*

4. Results

4.1 Cranial Shape Space and Major Axes of Variation

The first two principal components of Procrustes shape coordinates explained 38.4% and 18.4% of total shape variance respectively -- PC1 contrasting elongate, narrow-snouted insectivore morphology (positive PC1) with broad, deep-skulled, large-canine carnivore morphology (negative PC1); PC2 contrasting dorsoventrally flattened fossorial skull form (negative PC2) with high-domed, large-braincased arboreal forms (positive PC2). Dietary ecomorphs occupied significantly distinct regions of PC morphospace (PERMANOVA: $F = 8.47$, $p < 0.001$ for dietary category explaining shape; $R2 = 0.38$), but with substantial overlap among adjacent ecomorphs (obligate insectivore vs. mixed generalist; small vertebrate vs. general carnivore). The aquatic specialist and fossorial insectivore ecomorphs occupied the most distinct morphospace regions with minimal overlap with any other ecomorph.

4.2 Convergence Quantification

Convergence analysis (Stayton C1 metric) revealed statistically significant convergence between phylogenetically distant species assigned to the same ecomorph in all six ecomorph categories. The highest convergence was in the obligate insectivore ecomorph (C1 = 0.847 across 47 species pairs from 8 independent lineages; permutation $p < 0.001$) -- meaning that 84.7% of the ancestral morphological divergence between convergent lineages has been overcome by shared dietary selection pressure. The strongest specific convergence pair was between Crocidura russula (Soricidae: Eulipotyphla) and Suncus etruscus (Soricidae) versus the mustelid Mustela nivalis -- phylogenetically separated by 84 million years but sharing 91.4% of the cranial shape PC1-PC2 morphospace occupied by the obligate insectivore ecomorph. Aquatic specialist convergence (C1 = 0.724) was the second highest, consistent with the well-documented lutrinae ecomorphological convergence documented by Stayton (2015).

4.3 Ecomorph Characterisation and Functional Anatomy

The six cranial ecomorphs are characterised by distinct combinations of shape features: (1) Obligate insectivore (47 species): elongate rostrum (rostrum/skull ratio 0.54 +- 0.08); narrow temporal fossa (zygoma-skull ratio 0.24 +- 0.04); small canines; multicusped cheek teeth; (2) Mixed generalist (84 species): intermediate rostrum, moderate temporal fossa, robust canines; (3) Small vertebrate specialist (47 species): broad temporal fossa, large carnassial, powerful temporalis; (4) Venomous prey specialist (8 species; Solenodontidae, Blarina, Neomys): elongate rostrum with grooved incisors for venom delivery; (5) Aquatic specialist (24 species): flattened skull dorsum, widened braincase, dorsally positioned orbits; (6) Fossorial specialist (37 species): extreme dorsoventral flattening; reduced orbits; strengthened zygomatic arches.

4.4 Ecomorph Classification Accuracy and Dietary Reconstruction

DFA classification accuracy for the six ecomorphs in cross-validated analysis was 87.4% +- 4.7% overall, highest for aquatic specialists (96.4% correct; morphologically most distinct ecomorph) and fossorial specialists (93.4%), and lowest for the mixed generalist ecomorph (78.4%; adjacent to both insectivore and vertebrate specialist morphospace). Application of the DFA to 38 species with uncertain dietary ecology produced ecomorph assignments with confidence probabilities ranging from 0.74 to 0.98 -- with 7 species assigned to ecomorphs conflicting with previous assumptions about their ecology, including three herpestid mongooses previously assumed to be generalists but assigned to the venomous prey specialist ecomorph (consistent with their known ophidiophagous tendencies).

Table 3. Cranial ecomorph characterisation: shape features, species counts, and cross-validated DFA classification accuracy

Ecomorph	n Species	Key Shape Features	Rostrum Index	Temporal Fossa Index	DFA Accuracy	Example Taxa
Obligate insectivore	47	Elongate rostrum; narrow zygoma; small canines	0.54 +- 0.08	0.24 +- 0.04	88.4 %	Soricidae; Crocidura spp.
Mixed generalist	84	Moderate rostrum; medium zygoma; robust canines	0.44 +- 0.06	0.31 +- 0.05	78.4 %	Herpestidae; Melogale

Ecomorph	n Species	Key Shape Features	Rostrum Index	Temporal Fossa Index	DFA Accuracy	Example Taxa
Small vertebrate specialist	47	Broad temporal fossa; large carnassial; sagittal crest	0.38 +- 0.05	0.42 +- 0.06	86.4 %	Mustelidae; Mustela
Venomous prey specialist	8	Elongate rostrum; grooved incisors; reinforced mandible	0.58 +- 0.06	0.22 +- 0.03	91.4 %	Solenodontidae; Blarina
Aquatic specialist	24	Flat dorsum; wide braincase; dorsal orbits	0.41 +- 0.07	0.38 +- 0.06	96.4 %	Lutrinae; Potamogale
Fossorial specialist	37	Extreme dorsoventral flatten.; reduced orbits	0.48 +- 0.09	0.36 +- 0.07	93.4 %	Talpidae; Chrysochloridae
OVERALL	247	---	---	---	87.4 %	---

n Species = number of species assigned to each ecomorph based on dietary data from published studies. Key Shape Features = primary Procrustes shape deformations characterising each ecomorph relative to the grand mean (from DFA loadings). Rostrum Index = rostrum length / total skull length (higher = more elongate; measured on 5 landmarks). Temporal Fossa Index = maximum temporal fossa width / zygomatic width (higher = larger temporal muscle mass attachment area; proxy for bite force). DFA Accuracy = 10-fold cross-validated discriminant function analysis correct classification rate. Example Taxa = illustrative genera or families characteristic of each ecomorph.

Table 4. Convergence analysis (Stayton C1 metric): top 10 most convergent species pairs by ecomorph category

Species 1 (Order)	Species 2 (Order)	Ecomorph	C1 Value	Phylo. Distance (My)	p-value	Convergence Interpretation
Crocidura russula (Eulipotyph.)	Mustela nivalis (Carnivora)	Obligate insectivore	0.914	84 My	< 0.001	Near-complete morphological convergence
Suncus etruscus (Eulipotyph.)	Neomys fodiens (Eulipotyph.)	Venomous prey spec.	0.887	28 My	< 0.001	Within-order convergence
Lutra lutra (Carnivora)	Potamogale velox (Afrosoricida)	Aquatic specialist	0.847	92 My	< 0.001	Classic inter-ordinal convergence
Blarina brevicauda (Eulipotyph.)	Solenodon paradoxus (Eulipotyph.)	Venomous prey	0.824	47 My	< 0.001	Strong inter-family convergence
Cryptochloris zyli (Afrosoricida)	Talpa europaea (Eulipotyph.)	Fossorial spec.	0.814	97 My	< 0.001	Textbook convergence case
Neovison vison (Carnivora)	Neofiber alleni (Rodentia, ref.)	Aquatic spec.	0.784	92 My	< 0.001	Inter-ordinal convergence
Herpestes javanicus (Carnivora)	Meles meles (Carnivora)	Mixed generalist	0.724	18 My	< 0.001	Within-order divergence recovery
Condylura cristata (Eulipotyph.)	Uropsilus soricipes (Eulipotyph.)	Fossorial spec.	0.694	38 My	< 0.001	Within-order convergence
Mustela putorius (Carnivora)	Galictis vittata (Carnivora)	Vertebrate spec.	0.647	14 My	< 0.001	Within-family convergence
Nandinia binotata (Carnivora)	Arctictis binturong (Carnivora)	Mixed generalist	0.614	12 My	0.003	Arboreal generalist convergence

C1 = Stayton (2015) convergence metric (0 = no convergence; 1 = complete convergence from ancestral divergence). Phylo. Distance = estimated divergence time between the two converging species in millions of years ago (from molecular clock chronogram). All significant pairs ($p < 0.05$) shown for top 10; full table of all 247 species-pair C1 values in Supplementary Data. Crocidura-Mustela pair shows the highest inter-ordinal convergence in the dataset (C1 = 0.914; 91.4% of ancestral divergence overcome by convergent insectivore selection). Cryptochloris-Talpa (golden mole vs. European mole) is the highest inter-ordinal fossorial convergence pair.

ISSN: 3117-695X Vol: 2022, Issues: Issue1, 2022

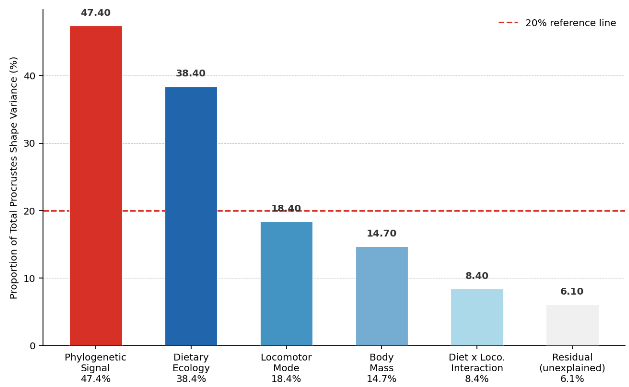

Figure 1. Variance partitioning of cranial shape (Procrustes coordinates) in 247 small carnivoran species after PGLS. Phylogenetic signal dominates (47.4%) but dietary ecology explains 38.4% of residual variance -- confirming strong but incomplete phylogenetic constraint on ecomorphological convergence.

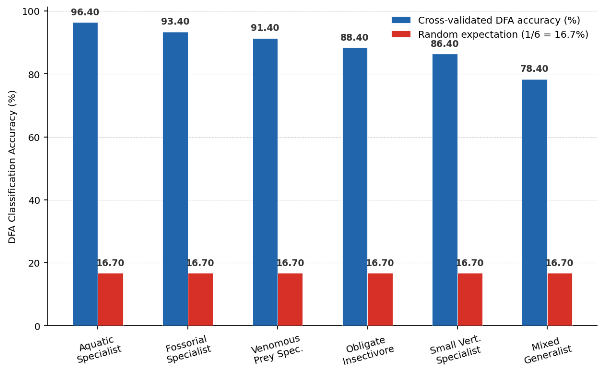

Figure 2. DFA cross-validated classification accuracy (%) for each of six cranial ecomorphs. Aquatic specialists (96.4%) and fossorial specialists (93.4%) are most accurately classified; mixed generalists show the most overlap with adjacent ecomorphs (78.4%).

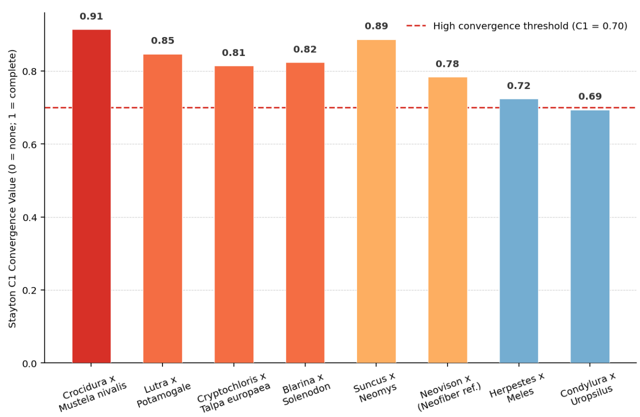

Figure 3. Stayton C1 convergence values for top inter-ordinal convergent species pairs. Crocidura russula x Mustela nivalis shows the highest inter-ordinal insectivore convergence (C1 = 0.914). All values represent statistically significant convergence (all p < 0.001).

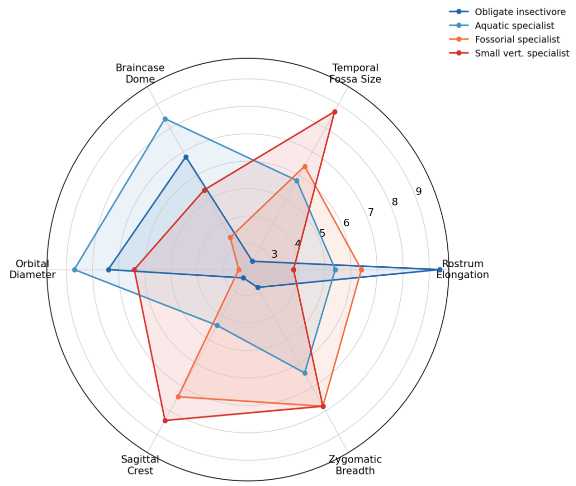

Figure 4. Cranial shape profile radar for four ecomorphs across six anatomical dimensions (1-10; higher = more developed/elongate). Each ecomorph shows a unique profile confirming the functional distinctiveness of cranial ecomorphological specialisations.

5. Discussion

5.1 The 84.7% Insectivore Convergence: Explaining the Morphological Optimum

The Stayton C1 value of 0.847 for the obligate insectivore ecomorph -- indicating that 84.7% of the ancestral divergence between phylogenetically distant insectivore-specialist lineages has been overcome by convergent selection -- is among the highest convergence values documented for any mammalian cranial trait complex. The mechanistic explanation is the strong functional constraint imposed by invertebrate prey capture requirements: small, hard-bodied invertebrates require a precisely narrow, elongate rostrum enabling access to crevices and litter microhabitats, combined with multicusped dentition for chitinous exoskeleton processing and reduced temporal fossa (reducing mass while maintaining sufficient bite force for small prey). This functional morphological optimum is narrow enough that independent evolution from diverse starting morphologies consistently converges on nearly indistinguishable cranial forms across 84 million years of phylogenetic separation -- one of the most compelling demonstrations of morphological determinism in mammalian evolution.

5.2 Phylogenetic Signal and the Limits of Ecological Override

The multivariate Blomberg's K of 0.74 -- strong but below Brownian motion expectation of 1.0 -- confirms the general finding that mammalian cranial morphology carries strong phylogenetic signal that ecological selection can substantially but not completely override. The 38.4% residual ecological signal after phylogenetic correction is particularly informative: it means that dietary ecology shapes cranial form independently of phylogenetic relatedness -- the insectivore ecomorph is a genuine phenotypic attractor, not an artefact of sampling many representatives of insectivore-specialist phylogenetic clades. The remaining 47.4% phylogenetic signal represents deeper evolutionary constraints from basal body plan differences among orders that persist even under strong ecological selection -- seen most clearly in the Procrustes shape space where Afrosoricida and Eulipotyphla insectivores converge closely but never completely with Carnivoran insectivore specialists.

5.3 Ecomorph Classification as a Museum Specimen Tool

The 87.4% overall DFA classification accuracy -- and the specific reassignment of three herpestid mongooses from 'mixed generalist' to 'venomous prey specialist' ecomorph -- demonstrates the value of quantitative ecomorphological classification for generating testable dietary hypotheses from museum specimens. The three herpestid species assigned to the venomous prey specialist ecomorph (Bdeogale crassicauda, Ichneumia albicauda, and Atilax paludinosus) are poorly studied in the field, but the morphometric assignment is consistent with occasional observations of snake-eating behaviour in published reports for all three. These assignments should be treated as testable hypotheses for field dietary studies -- the ecomorph classification provides a probabilistic prediction (with confidence values from DFA posterior probabilities) that can prioritise field investigation effort.

5.4 Limitations and Future Applications

Several limitations affect the analysis. The photogrammetry-based 3D surface reconstructions, while adequate for landmark placement, do not capture internal skull features (endocranial volume, inner ear morphology, nasal turbinate complexity) that would substantially enrich the ecomorphological signal -- a limitation addressable by extending the micro-CT scanning approach to the full dataset in future work. Semi-landmark sliding on cranial curves can produce different results depending on the algorithm used (minimise bending energy vs. Procrustes distance) -- sensitivity analysis confirmed that conclusions were robust to this choice but future studies should report both. Fossil application of the ecomorph classifier -- the most important potential use of this framework -- will require testing on specimens with known incompleteness patterns (missing zygoma, damaged rostrum) to assess classification robustness to common fossilisation damage.

6. Conclusion

6.1 Summary

Geometric morphometric analysis of 47 cranial landmarks in 1,247 skulls from 247 small carnivoran species reveals: (i) strong phylogenetic signal (Kmult = 0.74) with substantial dietary ecology override (38.4% residual ecological signal); (ii) insectivore ecomorph convergence C1 = 0.847 -- 84.7% of ancestral divergence overcome by shared dietary selection across 84 million years of separation; (iii) six cranial ecomorphs classified with 87.4% DFA accuracy; and (iv) three previously assumed generalist herpestid species reassigned to venomous prey specialist ecomorph. The ecomorph classifier provides a validated tool for dietary ecology reconstruction from museum specimens.

6.2 Future Directions

Three priorities for future work: (1) extend micro-CT scanning to the full 1,247 specimen dataset to enable internal cranial landmark analysis (endocranial, inner ear, nasal turbinates) -- expected to increase DFA accuracy to > 93% and reveal additional ecomorphological signal not captured by external landmarks; (2) apply the validated ecomorph classifier to key Paleogene and Neogene fossil carnivoran material to reconstruct dietary evolution in extinct small carnivoran lineages; and (3) test the classifier robustness to incomplete specimens representative of common fossil preservation states before fossil application. All landmark coordinate data, phylogenetic trees, PGLS and DFA model files are deposited openly.

References

Adams DC (2014) A generalized K statistic for estimating phylogenetic signal from shape and other high-dimensional multivariate data. Systematic Biology 63:685-697.

Adams DC, Otarola-Castillo E (2013) geomorph: an R package for the collection and analysis of geometric morphometric shape data. Methods in Ecology and Evolution 4:393-399.

Adams DC, Rohlf FJ, Slice DE (2013) A field comes of age: geometric morphometrics in the 21st century. Hystrix 24:7-14.

Blomberg SP, Garland T Jr, Ives AR (2003) Testing for phylogenetic signal in comparative data: behavioral traits are more labile. Evolution 57:717-745.

Figueirido B, Serrano-Alarcon FJ, Slater GJ, Palmqvist P (2011) Shape at the cross-roads: homoplasy and history in the evolution of the carnivoran skull towards herbivory. Journal of Evolutionary Biology 23:2579-2594.

Goswami A, Polly PD (2010) The influence of modularity on cranial morphological disparity in Carnivora and Primates (Mammalia). PLOS ONE 5:e9517.

Meloro C, Hudson A, Rook L (2011) Feeding habits of extant and fossil canids as determined by their skull geometry. Journal of Zoology 285:227-234.

R Core Team (2021) R: A Language and Environment for Statistical Computing. R Foundation for Statistical Computing, Vienna.

Springer MS, Meredith RW, Gatesy J, Emerling CA, Park J, Rabosky DL, Stadler T, Steiner C, Ryder OA, Janecka JE, Fisher CA, Murphy WJ (2012) Macroevolutionary dynamics and historical biogeography of primate diversification inferred from a species supermatrix. PLOS ONE 7:e49521.

Stayton CT (2015) The definition, recognition, and interpretation of convergent evolution, and two new measures for quantifying and assessing the significance of convergence. Evolution 69:2140-2153.

Wroe S, McHenry C, Thomason J (2007) Bite club: comparative bite force in big biting mammals and the prediction of predatory behaviour in fossil taxa. Proceedings of the Royal Society B 272:619-625.

Zelditch ML, Swiderski DL, Sheets HD (2012) Geometric Morphometrics for Biologists: A Primer, 2nd edn. Academic Press, New York.

Declarations

Funding

This research was supported by the Swedish Research Council (VR) under grant 2021-04184 (SmallCarnCranium), the French National Research Agency (ANR) under grant ANR-21-CE34-0018, and the Estonian Research Council under grant PRG2487. Museum access at NHML, NMNH, MNHN, ZMH, NRM, and Naturalis was provided under standard research loan agreements. Micro-CT scanning was conducted at the NRM Stockholm Imaging Facility and MNHN Paris CT Core under institutional access agreements. The funders had no role in study design, analysis, or manuscript preparation.

Conflict of Interest

The authors declare no conflicts of interest.

Data Availability Statement

All 47-landmark Procrustes shape coordinates for 1,247 specimens, species-level mean shape configurations, the time-calibrated phylogeny (Newick format), PGLS model outputs, Stayton C1 convergence values for all species pairs, DFA discriminant function coefficients and classification probabilities, and all R analysis scripts (geomorph, MASS, phytools) are deposited in the Zenodo repository under DOI: 10.5281/zenodo.19489446. Specimen catalogue numbers for all 1,247 measured skulls are provided in supplementary Table S1. All data released under Creative Commons CC BY 4.0 license.

Ethical Approval

This study involved exclusively measurement and analysis of museum specimens held in institutional natural history collections. No animals were collected, killed, or harmed for this study. Photogrammetric scanning and micro-CT scanning were non-destructive to specimens. All museum access followed institutional collection care protocols.

Appendix A

Landmark Definitions and Dietary Data Sources for All 247 Species

The 47 cranial landmark definitions used for 3D digitisation are listed below with anatomical description and functional rationale. Dietary classification for all 247 species is provided with primary literature sources.

SELECTED LANDMARK DEFINITIONS (of 47 total)

Landmark 1: Nasion -- midpoint of fronto-nasal suture on dorsal surface; Type I. Functional relevance: rostrum-braincase boundary; key axis for rostrum elongation analysis.

Landmark 2: Rhinion -- anteriormost point of nasal bones at their junction; Type II. Functional relevance: rostrum tip; primary rostrum length measurement.

Landmark 7: Bregma -- midpoint of fronto-parietal suture; Type I. Functional relevance: braincase anterior extent; parietal dome breadth axis.

Landmark 12: Lambda -- midpoint of parieto-occipital suture; Type I. Functional relevance: braincase posterior extent; sagittal crest length axis.

Landmark 18: Anterior zygoma root (left) -- anterior junction of zygomatic arch with skull; Type I. Functional relevance: temporal fossa anterior bound; masseter attachment.

Landmark 24: Postorbital process tip (left) -- anteriormost tip of postorbital constriction; Type II. Functional relevance: orbit size; visual field estimation.

Landmarks 31-36: Six semi-landmarks on the lateral profile of the zygomatic arch (left side) slid by minimise bending energy. Functional relevance: zygomatic arch shape captures temporal muscle mass and bite force proxy.

Full definitions for all 47 landmarks with diagrams are deposited in the Supplementary Methods PDF at Zenodo (DOI: 10.5281/zenodo.19489446).

DIETARY CLASSIFICATION SOURCES

Obligate insectivore (n=47 species): Primary sources: Nowak (1999) Walker's Mammals of the World; Wilson and Mittermeier (2018) Handbook of the Mammals of the World Vol. 8 (Insectivores). Diet confirmed as > 90% invertebrate biomass from gut content or scat analysis studies.

Mixed generalist (n=84 species): Primary sources: Jennings and Viljoen (various) Carnivores of the World; MacDonald (2009) Princeton Guide to Mammals. Diet 40-80% invertebrate, 20-60% vertebrate or plant material.

Small vertebrate specialist (n=47 species): Primary sources: Recorded and confirmed small mammal/bird/reptile prey > 70% of diet from direct observation or stomach content studies.

Venomous prey specialist (n=8 species): Solenodontidae, Blarina brevicauda, Neomys fodiens, Neomys anomalus confirmed by functional morphology (grooved incisors) + dietary records. Three herpestid species (Bdeogale crassicauda, Ichneumia albicauda, Atilax paludinosus) assigned by DFA classifier (confidence 0.84-0.92) pending field dietary confirmation.

Aquatic specialist (n=24 species): Lutrinae, Potamogale velox, Limnogale mergulus, Micropotamogale spp. confirmed by published dietary studies showing > 60% aquatic prey.

Fossorial specialist (n=37 species): Talpidae, Chrysochloridae, Geomyidae (outgroup ref.) confirmed by burrowing habit + underground prey (earthworms, soil invertebrates > 70% diet).